


How to Grow a Flat Leaf

Salem al-Mosleh¹ and L. Mahadevan^{1,2,*}

¹John A. Paulson School of Engineering and Applied Sciences, Harvard University, Cambridge, Massachusetts 02138, USA

²Departments of Physics, and Organismic and Evolutionary Biology, Harvard University, Cambridge, Massachusetts 02138, USA

 (Received 11 April 2022; accepted 8 May 2023; published 31 August 2023)

Growing a flat lamina such as a leaf is almost impossible without some feedback to stabilize long wavelength modes that are easy to trigger since they are energetically cheap. Here we combine the physics of thin elastic plates with feedback control theory to explore how a leaf can remain flat while growing. We investigate both in-plane (metric) and out-of-plane (curvature) growth variation and account for both local and nonlocal feedback laws. We show that a linearized feedback theory that accounts for both spatially nonlocal and temporally delayed effects suffices to suppress long wavelength fluctuations effectively and explains recently observed statistical features of growth in tobacco leaves. Our work provides a framework for understanding the regulation of the shape of leaves and other leaflike laminar objects.

DOI: [10.1103/PhysRevLett.131.098401](https://doi.org/10.1103/PhysRevLett.131.098401)

Shape is an emergent property of matter enabling function at every level in biology, from the molecular to the organismal. To ensure the robust generation of shape [1] in the (unavoidable) presence of noise, feedback mechanisms must couple sensing and growth [2–5]. This can be seen in the garden in plant leaves that are often flat [6,7], a configuration that is hard to achieve in thin growing laminae without feedback as they are susceptible to bending. In fact, recent studies in *N. tabacum* (tobacco) leaves show spatially correlated fluctuations of areal growth rate [8], consistent with an important role for feedback in maintaining this shape [9–13].

Motivated by these observations, here we propose a framework within which to study the control of thin surfaces, modeled as thin elastic plates that grow and change over time. We focus on small deviations from the flat state and study in-plane and across thickness growth (Fig. 1) and show that strain [14] and curvature [15,16] sensing together stabilize the flat state.

Mechanics of a growing lamina.—Motivated by the adaxial-abaxial polarity in leaves [17], we consider a thin plate with constant thickness h , where Young’s modulus is allowed to vary across the thickness (with average value E), and derive the corresponding reduced 2D elastic energy (see the Supplemental Material [18] Sec. S.1A and Refs. [19–21]). We assume that the plate (see the Supplemental Material [18], Sec. S.5 for results regarding shallow shells) is expanding exponentially with growth rate g , and its neutral surface (which may not coincide with the midsurface) is parametrized with Lagrangian coordinates taken to be the Cartesian coordinates $\mathbf{r} = (x_1, x_2)$ at time $t = 0$. The deviation from the flat state is described by the deflection $W(\mathbf{r}, t)$ of the neutral surface above the reference (x_1, x_2) plane (Fig. 1). For an isotropic material, there are

two elastic constants, E, ν in terms of which we can write a stretching stiffness $S = Eh$ that links the strain measures to the stress resultant $S_{ij}(\mathbf{r}, t)$. The scaled Airy stress function $\Phi(\mathbf{r}, t)$ is related to the stress tensor through $S_{11} = S\partial_2\partial_2\Phi$,

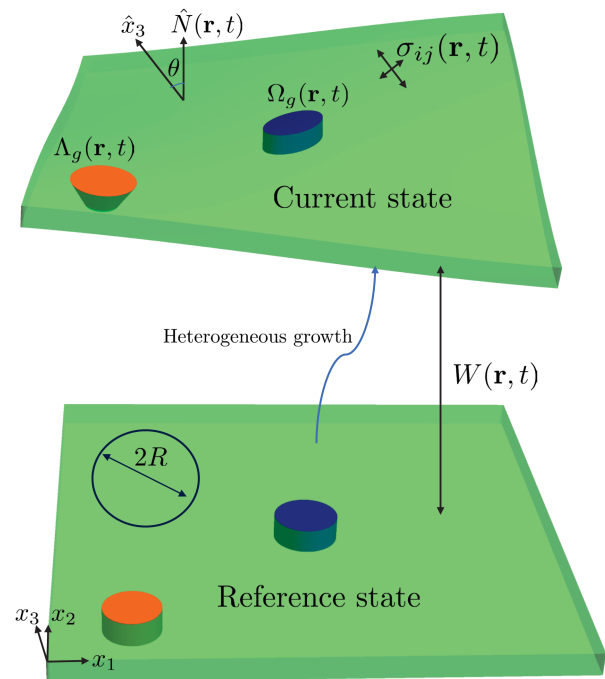


FIG. 1. Schematic of a growing, nearly flat, thin elastic plate. The shape of the leaf results from the inhomogeneous growth both in the in-plane [encoded by $\Omega_g(\mathbf{r}, t)$] and out-of-plane [encoded by $\Lambda_g(\mathbf{r}, t)$] directions. The shell is described by the out-of-plane deflection $W(\mathbf{r}, t)$ and the scaled Airy stress function (see text). The unit vector \hat{x}_3 points in the vertical direction, and $\hat{N}(\mathbf{r}, t)$ is the normal to the surface. The angle between them is $\theta(\mathbf{r}, t)$. R is the size of a region over which we coarse grain measurement of growth.

$S_{22} = S\partial_1\partial_1\Phi$, and $S_{12} = -S\partial_1\partial_2\Phi$. The Laplacian of the scaled Airy stress function satisfies $S\Delta\Phi(\mathbf{r}, t) = S_{11} + S_{22}$ and is proportional to the areal strain.

Since growth-induced elastic frustration leads to rapid equilibration (at the speed of sound) while feedback from strains that modulate growth is generally slow (due to the timescales over which these signals are transduced biochemically), the in-plane and out-of-plane growth are treated quasistatically. Then, at linear order we can describe an elastic plate using the depth-averaged compatibility and transverse force balance equations [22] as

$$\Delta^2\phi(\mathbf{r}, t) = \Omega_g(\mathbf{r}, t) \quad (1)$$

$$h\Delta^2w(\mathbf{r}, t) = \Lambda_g(\mathbf{r}, t), \quad (2)$$

where $\Omega_g(\mathbf{r}, t)$ reflects the incompatibility due to in-plane growth, and $\Lambda_g(\mathbf{r}, t)$ is due to curvature growth (see Fig. 1 and Ref. [22]). We defined $w(\mathbf{r}, t) \equiv e^{-gt}W(\mathbf{r}, t)$, and $\phi(\mathbf{r}, t) \equiv e^{-gt}\Phi(\mathbf{r}, t)$ to facilitate calculations in Fourier space on a growing background, and dimensional analysis demands that the coefficient of $\Delta^2w(\mathbf{r}, t)$ be a factor $O(h)$ smaller than the corresponding coefficient of $\Delta^2\phi(\mathbf{r}, t)$.

Local and instantaneous feedback.—Our goal is to study the stability of the flat, stress-free state. At linear order, the most general form of the feedback law that we can write to account for the slow feedback from shape to growth leads to (see the Supplemental Material [18], Secs. S.2A and S.2B for details of other equivalent forms written in terms of geometric quantities such as the first and second fundamental forms [23])

$$\partial_t\Omega_g = \int_{-\infty}^t dt' d^2\mathbf{r}' [G_{11}\Delta^2\phi + G_{12}h\Delta^2w(\mathbf{r}', t')], \quad (3)$$

$$\partial_t\Lambda_g = \int_{-\infty}^t dt' d^2\mathbf{r}' [G_{21}\Delta^2\phi + G_{22}h\Delta^2w(\mathbf{r}', t')], \quad (4)$$

where $G_{ij}(\mathbf{r} - \mathbf{r}', t - t')$ are the feedback kernels that represent the (possibly nonlocal and delayed) coupling of growth to the state of the system described in terms of the inhomogeneous in-plane growth $\Delta^2\phi(\mathbf{r}', t')$ (analogous to the Gauss curvature or the Ricci scalar) and $\Delta^2w(\mathbf{r}', t')$ (analogous to a transverse pressure). As for Eq. (2), dimensional analysis requires the coefficients of $\Delta^2w(\mathbf{r}, t)$ be a factor $O(h)$ smaller than the corresponding coefficients of $\Delta^2\phi(\mathbf{r}, t)$.

The terms proportional to $G_{12}(\boldsymbol{\rho}, \tau)$ and $G_{21}(\boldsymbol{\rho}, \tau)$ —which couple in-plane and out-of-plane growth—are only allowed for systems that violate the symmetry $\hat{N} \rightarrow -\hat{N}$, where $\hat{N}(\mathbf{r}, t)$ is the normal to the midsurface. This is the case for leaves possessing adaxial-abaxial polarity, which is important for the proper growth of a flat leaf blade [24]. In such cases, different proliferation rates on the abaxial and adaxial sides [25,26] lead to curved leaf phenotypes.

The simplest choice of kernel corresponds to the case of local feedback—where the instantaneous rate of expansion and shear due to growth is a function of local variables such as curvature and strain (see the Supplemental Material [18], Sec. S.2A)—and is described using the Dirac delta function by

$$G_{ij}(\boldsymbol{\rho}, \tau) = -\alpha_{ij}\delta(\tau)\delta(\boldsymbol{\rho}), \quad (5)$$

where the feedback matrix α_{ij} , with units of time^{-1} , is not required to be symmetric. To understand the stability of a nominally flat plate to perturbations of growth, we substitute the ansatz $\phi(\mathbf{r}, t) = \phi_0 e^{i\mathbf{q}\cdot\mathbf{r} + \lambda t}$ and $w(\mathbf{r}, t) = w_0 e^{i\mathbf{q}\cdot\mathbf{r} + \lambda t}$ into Eqs. (1)–(5), which gives two eigenvalue solutions for the growth, given by

$$\lambda_{\pm}(\mathbf{q}) = -\frac{1}{2} \left(\text{tr}[\alpha] \pm \sqrt{\text{tr}[\alpha]^2 - 4 \det[\alpha]} \right), \quad (6)$$

where $\text{tr}[\alpha]$ and $\det[\alpha]$ are the trace and determinant of the feedback matrix α_{ij} . Note that the growth rates are independent of wave number \mathbf{q} , and therefore independent of system size L , consistent with the local nature of the growth law.

The system will be stable when $\text{Re}\lambda_{\pm}(\mathbf{q}) < 0$, which happens when $\det[\alpha] < 0$, $\text{tr}[\alpha] > 0$. When $4 \det[\alpha] > \text{tr}[\alpha]^2$ the system will be oscillatory but still stable. We note that stability requires both curvature and strain sensing, which ensures that $\det[\alpha] \neq 0$, and the lamina needs to be able to measure or sense deviations from the target flat, stress-free state driven by both curvature and in-plane growth.

However, while local and instantaneous feedback can lead to asymptotic stability of the flat state, we now show that this form of feedback is not efficient at suppressing stochastic fluctuations at the scale of the system size L . To see this, we extend Eqs. (3) and (4) and add stochastic terms to represent the effects of fluctuations in in-plane and curvature growth rate. Motivated by the variability of growth rate in developing leaves between cells at nearby positions and for the same cell at different times [27], we assume that fluctuations in in-plane areal growth, written as $\Delta\chi_{\phi}(\mathbf{r}, t)$, and curvature growth, written as $\Delta\chi_w(\mathbf{r}, t)$ that appear through the variations in the metric and curvature tensor (and scaled by a factor e^{-gt} as described in the Supplemental Material [18], Sec. S.2A) have a white noise spectrum so that

$$\langle \Delta\chi_{\phi}(\mathbf{r}, t) \Delta\chi_{\phi}(\mathbf{r}', t') \rangle = D_{\phi} \delta(\mathbf{r} - \mathbf{r}') \delta(t - t') \quad (7)$$

$$\langle \Delta\chi_w(\mathbf{r}, t) \Delta\chi_w(\mathbf{r}', t') \rangle = D_w \delta(\mathbf{r} - \mathbf{r}') \delta(t - t') \quad (8)$$

with D_ϕ, D_w being the noise strengths. For the case of local and instantaneous feedback given by Eq. (5), the stochastic version of Eqs. (3) and (4) can then be written as

$$\partial_t \Delta^2 \phi(\mathbf{r}, t) = -\alpha \Delta^2 \phi(\mathbf{r}, t) + \Delta^2 \chi_\phi(\mathbf{r}, t), \quad (9)$$

$$\partial_t \Delta^2 w(\mathbf{r}, t) = -\alpha \Delta^2 w(\mathbf{r}, t) + \Delta^2 \chi_w(\mathbf{r}, t), \quad (10)$$

where we substituted Eqs. (1) and (2) to rewrite the left-hand side and assumed, for simplicity, that $\alpha_{ij} = \alpha \delta_{ij}$ with δ_{ij} being the Kronecker delta (see the Supplemental Material [18], Sec. S.4A for the general case).

To understand deviations from planarity of the growing lamina, it is natural to consider the fluctuations of the angle between the surface normal $[\hat{N}(\mathbf{r}, t)]$ and the vertical (\hat{x}_3), which is given by $|\theta(\mathbf{r}, t)| \equiv |\cos^{-1}[\hat{N}(\mathbf{r}, t) \cdot \hat{x}_3]| \approx |\nabla w(\mathbf{r}, t)|$. In Fourier space, the linear Eqs. (8) and (9) lead to

$$i\omega \hat{w}(\mathbf{q}, \omega) = -\alpha \hat{w}(\mathbf{q}, \omega) + \hat{\chi}_w(\mathbf{q}, \omega), \quad (11)$$

$$\langle \hat{\chi}_w(\mathbf{q}, \omega) \hat{\chi}_w^\dagger(\mathbf{q}', \omega') \rangle = \frac{(2\pi)^3 D_w}{\mathbf{q}^4} \delta(\mathbf{q} - \mathbf{q}') \delta(\omega - \omega'), \quad (12)$$

where $\hat{\chi}_w^\dagger$ denotes complex conjugation, and the Fourier transform of a function $F(\mathbf{r}, t)$ is given by $\hat{F}(\mathbf{q}, \omega) = \int d^2\mathbf{r} dt e^{-i\mathbf{q}\cdot\mathbf{r} - i\omega t} F(\mathbf{r}, t)$. This allows us to calculate the strength of the angle fluctuations as

$$\begin{aligned} \langle \theta(\mathbf{r}, t)^2 \rangle &\approx \langle \nabla w(\mathbf{r}, t)^2 \rangle \\ &= \int \frac{d^2\mathbf{q}' d\omega'}{(2\pi)^3} \frac{d^2\mathbf{q} d\omega}{(2\pi)^3} (\mathbf{q} \cdot \mathbf{q}') \langle \hat{w}(\mathbf{q}, \omega) \hat{w}^\dagger(\mathbf{q}', \omega') \rangle. \end{aligned} \quad (13)$$

Assuming fluctuations are cut off for physical wavelengths smaller than thickness h and larger than system size $L(t)$, we solve Eq. (11) for $w(\mathbf{q}, \omega)$, substitute it into Eq. (13), and use Eq. (12) to get

$$\langle \theta(\mathbf{r}, t)^2 \rangle = \int_{L^{-1}}^{h^{-1}} \frac{d^2\mathbf{q} d\omega}{(2\pi)^3} \mathcal{P}_\theta(\mathbf{q}, \omega), \quad (14)$$

where $\mathcal{P}_\theta(\mathbf{q}, \omega)$ is the power spectral density given by

$$\mathcal{P}_\theta(\mathbf{q}, \omega) = \frac{D_w}{\mathbf{q}^2(\alpha^2 + \omega^2)}. \quad (15)$$

The integral in Eq. (14) yields $\langle \theta^2(\mathbf{r}, t) \rangle \sim \log(L/h)$, i.e., the ordered flat state is unstable to growth fluctuations for large aspect-ratio laminae. This result does not change when we relax the diagonal assumption on α_{ij} (see the Supplemental Material [18], Sec. S.4A). In general the cutoffs in Eq. (14) are time dependent, and care must be taken when calculating the effect of short wavelength fluctuations as they get expanded to larger scales due to growth. In the Supplemental Material [18], Secs. S.4B

and S.4C, we show how to address this issue and show that using the temporal Fourier transform approach is valid for strong enough feedback ($\alpha > g$).

To further understand the local feedback regime, we next considered correlations in spatially distinct regions. In the planar growth case, recent work [13] has shown that the equal time correlation function for density perturbations, which are proportional to $\Delta\phi(\mathbf{r}, t)$ decays as a power law at large distances. This happens due to the effect of small scale (leaf thickness or cell size) correlations that get inflated to large distances during growth and leads to $\langle \Delta\phi(\mathbf{r}, t) \Delta\phi(\mathbf{r}', t) \rangle \sim |\mathbf{r} - \mathbf{r}'|^{-2(\alpha+g)/g}$ (see the Supplemental Material [18], Sec. S.4B). Because of the similarity between Eqs. (7) and (9) and Eqs. (8) and (10), the curvature fluctuations decay at a large distance with the same exponent, $|\mathbf{r} - \mathbf{r}'|^{-2(\alpha+g)/g}$. On the other hand, angle fluctuations behave as $\langle \theta(\mathbf{r}, t) \theta(\mathbf{r}', t) \rangle \sim |\mathbf{r} - \mathbf{r}'|^{-2\alpha/g}$ (see the Supplemental Material [18], Sec. S.4B).

Nonlocal and delayed feedback.—Next, we ask whether alternative modes of feedback, e.g., those that allow for nonlocal coupling in space and time, can alleviate the problem of stabilizing the flat state (at linear order).

Perturbations from the flat reference state cause cells to produce long-range signaling molecules with a delay time scale assumed to be Γ^{-1} ; these propagate diffusively throughout the leaf. Then, a natural model for signal propagation associated with feedback is given by the diffusion equation, whose Green's function satisfies

$$\partial_t G_D(\boldsymbol{\rho}, \tau) - \mathcal{D} \Delta G_D(\boldsymbol{\rho}, \tau) = \mathcal{D} \delta(\boldsymbol{\rho}) e^{-\Gamma \tau}, \quad (16)$$

where \mathcal{D} is a diffusion constant (see the Supplemental Material [18], Sec. S.2B for effects of signal degradation). The signal described by $G_D(\boldsymbol{\rho}, \tau)$ is thought to be propagated in plants by the hormone auxin, which helps regulate growth and biomechanical patterns during morphogenesis [28–32]. These long-range signals [33,34] propagate faster than growth speeds [35] but much slower than the speed elastic equilibration, so that their effect may be integrated over developmental time [36] and play a role in leaf size control [37].

Using the spreading rate of the hormone auxin, we estimate $\mathcal{D} \approx 10 \text{ mm}^2/\text{hour}$ [38], which, along with $L \sim 1 \text{ cm}$ and $g \sim 0.01/\text{hour}$ [8], gives $gL^2/\mathcal{D} \sim 0.1 \ll 1$. Solving Eq. (16) in this quasistatic limit and using Green's function which satisfies $\Delta G_\Delta(\mathbf{r} - \mathbf{r}') = -\delta(\mathbf{r} - \mathbf{r}')$ replaces the local feedback law in Eq. (5) with

$$G_{ij}(\boldsymbol{\rho}, \tau) = -\alpha_{ij} \delta(\tau) \delta(\boldsymbol{\rho}) - \frac{g e^{-\Gamma \tau}}{h^2} \beta_{ij} G_\Delta(\boldsymbol{\rho}), \quad (17)$$

where g^{-1} is the timescale of growth, α_{ij} is a feedback matrix corresponding to the local contribution, β_{ij} gives the nonlocal contribution, and both have units of time^{-1} .

Choosing $\alpha_{ij} = \alpha\delta_{ij}$, $\beta_{ij} = \beta\delta_{ij}$ for simplicity and plugging Eq. (17) into Eqs. (3) and (4) we get the modified system accounting for nonlocal, delayed feedback as

$$\partial_t \Delta^2 \phi(\mathbf{r}, t) = \Delta^2 \chi_\phi(\mathbf{r}, t) - \alpha \Delta^2 \phi(\mathbf{r}, t) + \frac{g\beta}{h^2} \int_{-\infty}^t e^{-\Gamma(t-t')} \Delta \phi(\mathbf{r}, t') dt', \quad (18)$$

$$\partial_t \Delta^2 w(\mathbf{r}, t) = \Delta^2 \chi_w(\mathbf{r}, t) - \alpha \Delta^2 w(\mathbf{r}, t) + \frac{g\beta}{h^2} \int_{-\infty}^t e^{-\Gamma(t-t')} \Delta w(\mathbf{r}, t') dt', \quad (19)$$

where we used Eqs. (1) and (2) and integrated by parts to obtain the Laplacian feedback appearing on the right-hand sides. Here the stochastic terms $\Delta^2 \chi_w(\mathbf{r}, t)$ and $\Delta^2 \chi_\phi(\mathbf{r}, t)$ are assumed to satisfy Eqs. (7) and (8) as in the local feedback case.

To understand the stability of the flat state to variations in the growth rates, we use the ansatz $\phi(\mathbf{r}, t) = \phi_0 e^{i\mathbf{q}\cdot\mathbf{r} + \lambda t}$ and $w(\mathbf{r}, t) = w_0 e^{i\mathbf{q}\cdot\mathbf{r} + \lambda t}$ and substitute into Eqs. (18) and (19). We then find that the deterministic part of the equation gives

$$\lambda = -\alpha - \frac{g\beta}{h^2 \mathbf{q}^2 \Gamma + \lambda}. \quad (20)$$

When the nonlocal feedback contribution $\beta = 0$ we get $\lambda = -\alpha$, as expected from Eq. (6) with $\alpha_{ij} = \alpha\delta_{ij}$. When $\beta \neq 0$, we have two solutions given by

$$\lambda_{\pm}(\mathbf{q}) = -\frac{1}{2} \left(\alpha + \Gamma \pm \sqrt{(\alpha - \Gamma)^2 - \frac{4\beta g}{h^2 \mathbf{q}^2}} \right), \quad (21)$$

where the contribution of the nonlocal term β dominates for long wavelengths ($\mathbf{q}^2 \ll 4\beta g/h^2 \alpha^2$), but is negligible for short wavelengths ($\mathbf{q}^2 \gg 4\beta g/h^2 \alpha^2$). We see that the flat configuration is stable only when $\alpha > 0$ (in the limit $\mathbf{q}^2 \rightarrow \infty$, $\lambda_+ = -\alpha$ and $\lambda_- = -\Gamma$) and $\beta > 0$ (otherwise when $\mathbf{q}^2 \rightarrow 0$ one can get a positive growth rate). In Fig. 2, we show the boundary of the stable parameter region indicated by whether the unstable mode has a large ($|q| \sim L^{-1}$) or small wavelength ($|q| \sim h^{-1}$), which may correspond to different phenotypes of mutant leaves [25,39]. For long wavelengths, Eq. (21) leads to oscillations on the way to the flat state, which may be related to the observed fluttering behavior in leaves during development [40].

To understand how fluctuations modify the deterministic feedback dynamics considered above, we start by writing the out-of-plane response of the plate Eq. (19) in Fourier space as

$$i\omega \hat{w} = \hat{\chi}_w(\mathbf{q}, \omega) - \left(\alpha + \frac{g\beta}{h^2 \mathbf{q}^2 \Gamma + i\omega} \right) \hat{w}(\mathbf{q}, \omega). \quad (22)$$

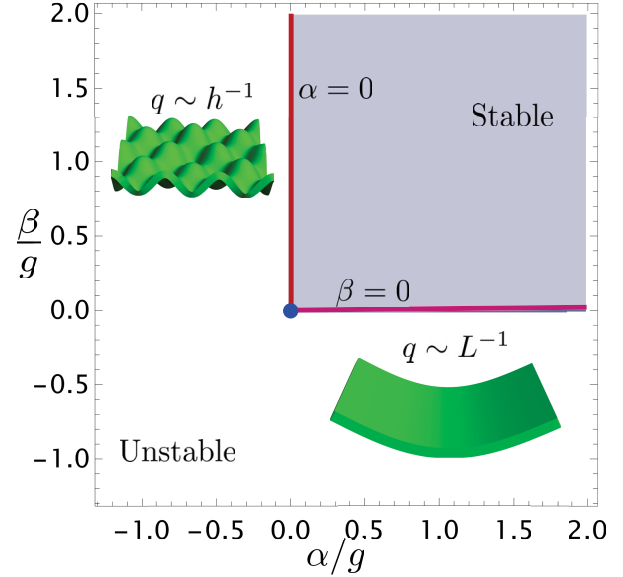


FIG. 2. Stability phase diagram. The phase diagram corresponding to Eq. (21). The thick lines represent the boundary of the stable region which are in turn divided according to whether the first unstable modes are large ($|\mathbf{q}| \sim L^{-1}$) or small ($|\mathbf{q}| \sim h^{-1}$) deformations. The blue points where the two boundaries meet correspond to no feedback $\alpha = \beta = 0$. The two types of unstable modes ($\alpha \sim 0$ or $\beta \sim 0$) are illustrated by the surfaces shown, and may explain phenotypes of mutant leaves [25,39].

Solving Eq. (22) for $\hat{w}(\mathbf{q}, \omega)$ and using Eq. (12), we get an expression for the power spectral density of the normal angle fluctuations given by Eq. (14) modified to account for nonlocal feedback that reads as

$$\mathcal{P}_\theta = \frac{(\omega^2 + \Gamma^2) \mathbf{q}^2 D_w}{\left((\omega^2 - \alpha\Gamma) \mathbf{q}^2 - \frac{g\beta}{h^2} \right)^2 + \mathbf{q}^4 (\alpha + \Gamma)^2 \omega^2}. \quad (23)$$

Unlike the case of local feedback (when $\beta = 0$) corresponding to Eq. (15), when $\beta \neq 0$, the spectral density $\mathcal{P}_\theta(\mathbf{q}, \omega)$ in Eq. (23) is well behaved in the long-wavelength limit and vanishes when $\mathbf{q}^2 = 0$. As a result, angle fluctuations remain finite, $\langle \theta(\mathbf{r}, t)^2 \rangle \sim O(L^0)$, as $L \rightarrow \infty$. However, in contrast to the case of local feedback, the fluctuations described by Eq. (23) are not scale invariant [$\mathcal{P}_\theta(\mathbf{q}, \omega)$ is not a power law in \mathbf{q}^2].

To quantitatively compare our model to recent experiments [8], we look at the fluctuations in areal strain rate, $\mathcal{A}(\mathbf{r}, t) \approx \partial_t \epsilon_{ii}(\mathbf{r}, t)/2$, where ϵ_{ii} is the sum of elastic and growth strain tensors, (see the Supplemental Material, Sec. S.4D, and Ref. [22]). The average areal strain rate is defined as $\bar{\mathcal{A}}(\mathbf{r}, t) \equiv (1/\pi R^2) \int_{R'} \mathcal{A}(\mathbf{r}', t') d^2 \mathbf{r}'$, and its variance is defined as $\Sigma_{\mathcal{A}}(R)^2 \equiv \langle (\bar{\mathcal{A}}(\mathbf{r}, t) - \langle \bar{\mathcal{A}}(\mathbf{r}, t) \rangle)^2 \rangle$, coarse grained over discs of size R centered at the point \mathbf{r} (Fig. 1).

To calculate $\Sigma_{\mathcal{A}}(R)$ using our model, we note that $\mathcal{A}(\mathbf{r}, t) \sim \partial_t \Delta \phi(\mathbf{r}, t)$, since $E \Delta \phi(\mathbf{r}, t)$ is the trace of the

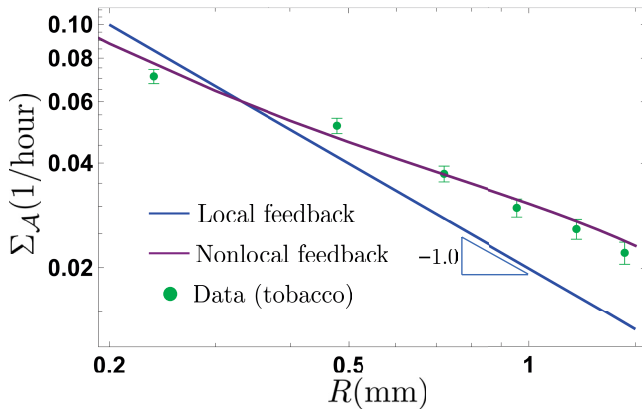


FIG. 3. Fluctuations in areal growth rate. A log-log plot of the standard deviation in areal strain rate Σ_A (in units of inverse hours), where $\mathcal{A}(\mathbf{r}, t) \approx \partial_i \epsilon_{ii}(\mathbf{r}, t)$ is averaged over a region of size R (see Fig. 1). Following Eq. (25), local feedback ($\beta = 0$) leads to $\Sigma_A \propto R^{-1}$ whereas purely nonlocal feedback ($\alpha = 0$) can be solved numerically with $g \approx 0.02/\text{hour}$ and $Tg \sim 0.01$ estimated from Ref. [8]; $h \approx 0.2$ mm from Ref. [42]; and $\beta/g = 40$, $\Gamma/g = 10$, and $D_\phi \approx 0.12h^2g$ chosen to fit the data taken from Ref. [8] (see the Supplemental Material, Sec. S.4E, for details of parameter fits). We note that the data extend to small length scales, close to the cutoff length $R \sim h \sim 0.2$ mm; for length scales below this cutoff, our thin-plate continuum model may not be valid.

elastic stress tensor. As Eq. (19) has a similar form to Eq. (18), we can repeat the steps leading to Eq. (23) (see the Supplemental Material, Secs. S.4C and S.4D, for subtleties associated with growth) to obtain the result

$$\Sigma_A^2 \propto \langle \partial_t \Delta \phi(\mathbf{r}, t)^2 \rangle \propto \int^{R^{-1}, T^{-1}} \frac{d^2 \mathbf{q} d\omega}{(2\pi)^3} \mathcal{P}_A(\mathbf{q}, \omega), \quad (24)$$

$$\mathcal{P}_A \propto \frac{\omega^2(\omega^2 + \Gamma^2) \mathbf{q}^4 D_\phi}{\left((\omega^2 - \alpha\Gamma) \mathbf{q}^2 - \frac{\beta g}{h^2} \right)^2 + \mathbf{q}^4 (\alpha + \Gamma)^2 \omega^2}, \quad (25)$$

where the \mathbf{q} integral is cutoff by R^{-1} due to spatial averaging over the disk of size R , T^{-1} is the high frequency cutoff (see the Supplemental Material, Sec. S.4D), and the additional factor of $\mathbf{q}^2 \omega^2$ compared with Eq. (23) is due to the different number of derivatives in $\partial_t \Delta \phi(\mathbf{r}, t)$ and $|\nabla w(\mathbf{r}, t)|$.

For purely local feedback ($\beta = 0$), $\mathcal{P}_A(\mathbf{q}, \omega) = \mathcal{P}_A(\omega)$ is independent of \mathbf{q} , and we obtain the power law $\Sigma_A \propto R^{-1}$ [as can be seen by changing coordinates $q \rightarrow Rq$ in the integral Eq. (24)]. This is consistent with prior results addressing stochastic growth in purely two-dimensional elastic tissues subject to local mechanical feedback [13] which showed that area changes in adjacent growing clones are uncorrelated. However, experiments on leaf growth [8] suggest that $\Sigma_A \propto R^{-p}$, $p \approx 0.61$ (Fig. 3), and differs from the R^{-1} behavior expected if growth (rate) fluctuations

were not correlated spatially. This indicates the need for a nonlocal feedback law embodied in Eqs. (3), (4), and (17) that would lead to long-range correlations in the fluctuation spectrum, similar to those predicted in models of mechano-responsive viscous tissue [41].

In contrast, for purely nonlocal feedback ($\alpha = 0$) Σ_A does not follow a power-law behavior in general [because the power spectral density is not scale invariant unless $\Gamma = 0$, whence we have to consider the range of the integral in Eq. (24) to ensure nondivergent behavior]. In Fig. 3, we show that results obtained by directly integrating Eq. (24) numerically with specific choices for the parameters (see figure caption and the Supplemental Material, Sec. S.4E, for details) are able to capture experimental observations [8].

Conclusion.—Our mathematical framework formalizes the intuition that growing a flat lamina stably is difficult because small fluctuations in metric and curvature growth are both destabilizing on long length scales. By coupling elasticity and strain-induced feedback in a linear setting we show that spatially nonlocal, temporally delayed feedback suppresses long wavelength fluctuations and furthermore captures experimentally observed scaling behavior for area fluctuations. Our analysis is a first step toward understanding the stable growth of flat lamina, and future work will explore the role of geometric nonlinearities combined with the subtleties that arise from the growing number of modes in growing systems.

We acknowledge partial financial support from a DARPA MURI grant MINT, the NSF-Simons Center for Mathematical and Statistical Analysis of Biology 1764269, the Simons Foundation and the Henri Seydoux Fund.

*lmahadev@g.harvard.edu

- [1] H. M. Meyer and A. H. Roeder, Stochasticity in plant cellular growth and patterning, *Front. Plant Sci.* **5**, 420 (2014).
- [2] J. Lempe, J. Lachowiec, A. M. Sullivan, and C. Queitsch, Molecular mechanisms of robustness in plants, *Curr. Opin. Plant Biol.* **16**, 62 (2013).
- [3] O. Hamant and B. Mouliia, How do plants read their own shapes?, *New Phytol.* **212**, 333 (2016).
- [4] P.-F. Lenne, E. Munro, I. Heemskerk, A. Warmflash, L. Bocanegra-Moreno, K. Kishi, A. Kicheva, Y. Long, A. Fruleux, A. Boudaoud *et al.*, Roadmap for the multiscale coupling of biochemical and mechanical signals during development, *Phys. Biol.* **18**, 041501 (2021).
- [5] B. Mouliia, S. Douady, and O. Hamant, Fluctuations shape plants through proprioception, *Science* **372** (2021).
- [6] G. Mitchison, Conformal growth of Arabidopsis leaves, *J. Theor. Biol.* **408**, 155 (2016).
- [7] K. Alim, S. Armon, B. I. Shraiman, and A. Boudaoud, Leaf growth is conformal, *Phys. Biol.* **13**, 05LT01 (2016).
- [8] S. Armon, M. Moshe, and E. Sharon, The multiscale nature of leaf growth fields, *Commun. Phys.* **4**, 122 (2021).

- [9] O. Hamant, M. G. Heisler, H. Jönsson, P. Krupinski, M. Uyttewaal, P. Bokov, F. Corson, P. Sahlin, A. Boudaoud, E. M. Meyerowitz *et al.*, Developmental patterning by mechanical signals in Arabidopsis, *Science* **322**, 1650 (2008).
- [10] A. Sampathkumar, P. Krupinski, R. Wightman, P. Milani, A. Berquand, A. Boudaoud, O. Hamant, H. Jönsson, and E. M. Meyerowitz, Subcellular and supracellular mechanical stress prescribes cytoskeleton behavior in Arabidopsis cotyledon pavement cells, *eLife* **3**, e01967 (2014).
- [11] O. Hamant, D. Inoue, D. Bouchez, J. Dumais, and E. Mjolsness, Are microtubules tension sensors?, *Nat. Commun.* **10**, 2360 (2019).
- [12] J. Chan and E. Coen, Interaction between autonomous and microtubule guidance systems controls cellulose synthase trajectories, *Curr. Biol.* **30**, 941 (2020).
- [13] O. K. Damavandi and D. K. Lubensky, Statistics of noisy growth with mechanical feedback in elastic tissues, *Proc. Natl. Acad. Sci. U.S.A.* **116**, 5350 (2019).
- [14] B. I. Shraiman, Mechanical feedback as a possible regulator of tissue growth, *Proc. Natl. Acad. Sci. U.S.A.* **102**, 3318 (2005).
- [15] J. Pulwicki, Dynamics of plant growth; a theory based on Riemannian geometry, [arXiv:1602.01778](https://arxiv.org/abs/1602.01778).
- [16] S. Al Mosleh, A. Gopinathan, and C. Santangelo, Growth of form in thin elastic structures, *Soft Matter* **14**, 8361 (2018).
- [17] K. Fukushima and M. Hasebe, Adaxial–abaxial polarity: The developmental basis of leaf shape diversity, *Genesis* **52**, 1 (2014).
- [18] See Supplemental Material at <http://link.aps.org/supplemental/10.1103/PhysRevLett.131.098401> for detailed derivations and generalizations of the results presented in this letter.
- [19] E. Efrati, E. Sharon, and R. Kupferman, Elastic theory of unconstrained non-Euclidean plates, *J. Mech. Phys. Solids* **57**, 762 (2009).
- [20] M. A. Dias, J. A. Hanna, and C. D. Santangelo, Programmed buckling by controlled lateral swelling in a thin elastic sheet, *Phys. Rev. E* **84**, 036603 (2011).
- [21] M. Lewicka, L. Mahadevan, and M. R. Pakzad, The föppl-von Kármán equations for plates with incompatible strains, *Proc. R. Soc. A* **467**, 402 (2011).
- [22] H. Liang and L. Mahadevan, The shape of a long leaf, *Proc. Natl. Acad. Sci. U.S.A.* **106**, 22049 (2009).
- [23] M. P. Do Carmo, *Differential Geometry of Curves and Surfaces: Revised and Updated Second Edition* (Courier Dover Publications, Mineola, NY, 2016).
- [24] R. Waites and A. Hudson, phantastica: A gene required for dorsoventrality of leaves in *Antirrhinum majus*, *Development* **121**, 2143 (1995).
- [25] J. Serrano-Cartagena, H. Candela, P. Robles, M. R. Ponce, J. M. Pérez-Pérez, P. Piqueras, and J. L. Micol, Genetic analysis of incurvata mutants reveals three independent genetic operations at work in Arabidopsis leaf morphogenesis, *Genetics* **156**, 1363 (2000).
- [26] H. Iwakawa, M. Iwasaki, S. Kojima, Y. Ueno, T. Soma, H. Tanaka, E. Semiarti, Y. Machida, and C. Machida, Expression of the ASYMMETRIC LEAVES2 gene in the adaxial domain of Arabidopsis leaves represses cell proliferation in this domain and is critical for the development of properly expanded leaves, *Plant J.* **51**, 173 (2007).
- [27] J. Elsner, M. Michalski, and D. Kwiatkowska, Spatiotemporal variation of leaf epidermal cell growth: A quantitative analysis of Arabidopsis thaliana wild-type and triple cyclinD3 mutant plants, *Ann. Bot.* **109**, 897 (2012).
- [28] D. Reinhardt, T. Mandel, and C. Kuhlemeier, Auxin regulates the initiation and radial position of plant lateral organs, *Plant Cell* **12**, 507 (2000).
- [29] D. Reinhardt, E.-R. Pesce, P. Stieger, T. Mandel, K. Baltensperger, M. Bennett, J. Traas, J. Friml, and C. Kuhlemeier, Regulation of phyllotaxis by polar auxin transport, *Nature (London)* **426**, 255 (2003).
- [30] M. G. Heisler, O. Hamant, P. Krupinski, M. Uyttewaal, C. Ohno, H. Jönsson, J. Traas, and E. M. Meyerowitz, Alignment between PIN1 polarity and microtubule orientation in the shoot apical meristem reveals a tight coupling between morphogenesis and auxin transport, *PLoS Biol.* **8**, e1000516 (2010).
- [31] W. A. Peer, J. J. Blakeslee, H. Yang, and A. S. Murphy, Seven things we think we know about auxin transport, *Mol. Plant* **4**, 487 (2011).
- [32] R. Bastien, S. Douady, and B. Mouliat, A unified model of shoot tropism in plants: Photo-, gravi- and proprioception, *PLoS Comput. Biol.* **11**, e1004037 (2015).
- [33] S. Johns, T. Hagihara, M. Toyota, and S. Gilroy, The fast and the furious: Rapid long-range signaling in plants, *Plant Physiol.* **185**, 694 (2021).
- [34] R. C. Reed, S. R. Brady, and G. K. Muday, Inhibition of auxin movement from the shoot into the root inhibits lateral root development in Arabidopsis, *Plant Physiol.* **118**, 1369 (1998).
- [35] E. M. Kramer, H. L. Rutschow, and S. S. Mabie, AuxV: A database of auxin transport velocities, *Trends Plant Sci.* **16**, 461 (2011).
- [36] C. S. Galvan-Ampudia, G. Cerutti, J. Legrand, G. Brunoud, R. Martin-Arevalillo, R. Azais, V. Bayle, S. Moussu, C. Wenzl, Y. Jaillais *et al.*, Temporal integration of auxin information for the regulation of patterning, *eLife* **9**, e55832 (2020).
- [37] K. Kawade, G. Horiguchi, and H. Tsukaya, Non-cell-autonomously coordinated organ size regulation in leaf development, *Development* **137**, 4221 (2010).
- [38] G. Mitchison, The shape of an auxin pulse, and what it tells us about the transport mechanism, *PLoS Comput. Biol.* **11**, e1004487 (2015).
- [39] M. Zhang, S. Huang, Y. Gao, W. Fu, G. Qu, Y. Zhao, F. Shi, Z. Liu, and H. Feng, Fine mapping of a leaf flattening gene Bralcm through BSR-Seq in Chinese cabbage (*Brassica rapa* L. ssp. *pekinensis*), *Sci. Rep.* **10**, 13924 (2020).
- [40] J. Derr, R. Bastien, É. Couturier, and S. Douady, Fluttering of growing leaves as a way to reach flatness: Experimental evidence on *Persea americana*, *J. R. Soc. Interface* **15**, 20170595 (2018).
- [41] A. Fruleux and A. Boudaoud, Modulation of tissue growth heterogeneity by responses to mechanical stress, *Proc. Natl. Acad. Sci. U.S.A.* **116**, 1940 (2019).
- [42] J. Dupuis, C. Holst, and H. Kuhlmann, Measuring leaf thickness with 3d close-up laser scanners: Possible or not?, *J. Imaging* **3**, 22 (2017).